EQUIJOST

Available online at www.equijost.com
Equity Journal of Science and Technology, 2021 8(1): 27 - 32
ISSN 2354-1814; E-ISSN 2682-5961
An Official Publication of Kebbi State University of Science and Technology, Aliero, Nigeria

Design and Simulation of an Advanced Solid-state Photomultiplier for Fiber-Optic Communication Systems

*[1]Sanusi K. Rabiu, [2]Salisu Musa, [1]Jerry Raymond
[1]Department of Telecommunication Engineering, Air Force Institute of Technology, Kaduna, Nigeria
[2]Department of Physics, Air Force Institute of Technology, Kaduna, Nigeria
*Corresponding Author's email: mumhafsat@gmail.com

Received: Feb 21, 2021: Accepted: Apr 18, 2021; Published Online: May 16, 2021

Abstract
Detection of weak infrared light is essential for high data rate fiber-optic communication systems since its performance depends heavily on the sensitivity and bandwidth of photodetectors. Semiconductor diodes are the most common types of photodetectors that are widely considered. Indium Arsenide (InAs), being an Avalanche Photodiode (APD), has become a solid-state photodetector of choice owing to its ability to detect infrared light of up to about 3.5 μm. In this work, the depletion width and electric field profile of p-i-n InAs were simulated and used to obtain the multiplication gain. The effect of combining a series of p-i-n InAs in order to obtain longer depletion width for the purpose of achieving high multiplication gain was investigated. To achieve this main target, the work was designed in two stages. The first stage involved designing a simple p-n junction of InAs to test the model. Further improvement of the design to increase the depletion region was carried out by sand-witching an intrinsic piece of semiconductor material between the p and n-regions to form p-i-n InAs. The results obtained showed that the modification led to an interesting increase in the depletion width, electric field and the multiplication gain. In the second stage, the series of p-i-n InAs were combined to form an "Advanced solid-state photomultiplier". For the first time, a larger depletion width was achieved and thus increased multiplication gain. The results presented deduced that this novel design is promising since an appreciable gain much greater than 1000 was achieved at about 6 V. Therefore, this could be used as an alternative to photomultiplier tube as well as other expensive photodetectors available.

Keywords: Design, Simulation, solid-state photomultiplier, communication systems

1. Introduction

The rapid spread and increased use of the internet has caused an upsurge in the demand for highly sensitive optical detectors for high data rate fiber optic communication systems [1,2]. Avalanche Photodiodes (APDs), owing to their small size, high quantum efficiency, internal current gain and high frequency response are now being considered for a wide range of other applications including Light Detection and Ranging (LIDAR), imaging for military applications, toxic gas sensing etc.[3-5]. In many of these applications, the optical signals reaching the photodiode may be low, necessitating some sort of amplification. Although external amplification through electronic circuits has been widely used, it can add significant noise which could affect the system's signal-to-noise ratio. Therefore, using light detectors that can offer internal amplification without adding much noise will significantly increase the system performance.

APDs, a p-n junction photodiode purposely made to be operated at high electric fields can achieve internal gain and low noise through impact ionization [1]. However, in most semiconductor devices, the impact ionization process does introduce some noise because it is a stochastics process [6,7]. While silicon APDs have excellent performance, they are limited to detecting wavelengths below one micron, and many of the applications described above require detection of weak infrared signals.

Mercury Cadmium Telluride (HgCdTe) avalanche photodiodes have been demonstrated to work very well at long infrared (7 – 12 μm) with high multiplication gain without significant excess noise but, as the composition is changed to allow shorter wavelength operation the gain decreases with an increase in excess noise [8]. Additionally, HgCdTe devices are excessively expensive due to high growth cost of the wafers and also require expensive coolers to keep the dark current to an acceptable level [9]. More recently indium arsenide (InAs) has been found to exhibit HgCdTe-like characteristics, with the potential to operate at high temperature and benefits from dramatically reduced substrate and epitaxial growth costs [9]. Thus, it could be used as an alternative to HgCdTe.

InAs, owing to its small energy bandgap of about 0.36 eV at room temperature, widely available, easy to grow, processed and can cover a wide range of wavelengths (up to about 3.5μm) has been considered as an alternative avalanche material for very low noise infrared APDs. In addition, it has achievable avalanche gain and excess noise behaviors that are highly similar to those of

https://dx.doi.org/10.4314/equijost.v8i1.4

HgCdTe APDs [10]. In this regard, several experimental and theoretical research efforts have been made to investigate the characteristics of this semiconductor material.

Mikhailova *et al*., [11] studied the ionization coefficients of InAs and concluded that both electron and hole carriers participate in the avalanche multiplication. However, the Monte Carlo calculations by Brenna and Mansur [12] indicated that the electron ionization coefficient values should be higher. In their study, Marshall *et al*., [13] conducted a systematic study on impact ionization, avalanche multiplication and excess noise of same semiconductor material and concluded that the material can only demonstrate HgCdTe characteristics if the avalanche multiplication is initiated by electrons. Sandall *et al*., [10] conducted analytical band Monte Carlo simulations to investigate the temperature dependence of impact ionization of same material. Their results showed an excellent agreement with the available experimental data for both avalanche gain and excess noise factors at various temperatures.

To date, there have been several experimental and theoretical works on the impact ionization, avalanche gain, temperature dependency etc. of this semiconductor material. In many materials, for a system to achieve higher gains, the external voltage (and hence e-field) can be increased. However, it has been shown that in InAs when the e-field exceeds a value around 70 kV/cm band to band tunneling occurs which significantly degrades the performance. Although, an alternative approach to obtaining high gain while maintaining a modest e-field and increasing the depletion width has been demonstrated, it is very challenging to maintain the high quality crystal growth for thickness >5 μm [14]. Therefore, this work aims at designing an advanced solid-state photomultiplier by combining series of InAs to increase the depletion region as well as to have sufficient e-field to initiate impact ionization process and at the same time avoid band-band tunneling.

2. Materials and Method

2.1 Simulation Parameters and Assumptions

The simulation parameters used in this work include standard electronic charge in coulombs (C), constant donor and acceptor doping concentrations per cm^3 and a varying applied reverse bias voltage in volts (V). Furthermore, since the material used is InAs, the dielectric constant, number of atoms in cm^3 and all other basic parameters such as lattice constant, electron affinity, optical phonon energy, density, effective electron and hole masses, were all that of InAs and assumed at room temperatures.

2.2 The Design Equations

The space-charge distribution and electrostatic potential of a p-n diode Ψ is given by the Poisson's equation [15]:

$$\frac{d^2\Psi}{dx^2} = -\frac{d\mathcal{E}}{dx} = -\frac{\rho_s}{\varepsilon_s} = -\frac{q}{\varepsilon_s}(N_D - N_A - p - n) \quad (1)$$

where, N_D and N_A are the doping concentration of p-side and n-side, ε_s is the permittivity of the material and q is the electronic charge.

For the region far away from the metalogical junction, the total space density is zero i.e., $\frac{d^2\Psi}{dx^2} = 0$ and $(N_D - N_A - p - n) = 0$ (2)

Therefore, the electrostatic potential of the p-type region is obtained by setting $N_D = n = 0$ in equation 2.

$$\Psi_p = -\frac{KT}{q} In\left(\frac{N_A}{n_i}\right)$$

$$\Psi_n = -\frac{KT}{q} In\left(\frac{N_A}{n_i}\right)$$

Thus, the total electrostatic potential difference between p-side and n-side neutral regions also known as built-in potential at room temperature is given by:

$$V_{ib} = \Psi_p - \Psi_p = \frac{KT}{q} In\left(\frac{N_A N_D}{n_i^2}\right) \quad (3)$$

Alternatively, the space-charge distribution and electrostatic potential can also be obtained from equation (1) by setting p = n = 0.

$$\frac{d^2\Psi}{dx^2} = -\frac{q}{\varepsilon_s}(N_D - N_A) \quad (4)$$

Thus,

$$\frac{d^2\Psi}{dx^2} = -\frac{q}{\varepsilon_s} N_D \quad \text{for} \quad -x_p \le x < 0 \quad (6)$$

$$\frac{d^2\Psi}{dx^2} = \frac{q}{\varepsilon_s} N_A \quad \text{for} \quad 0 < x \le x_n \quad (7)$$

The electric field is obtained by integrating equation 6 and 7:

$$\mathcal{E}(x) = -\frac{d\Psi}{dx} = -\frac{qN_A(x+x_p)}{\varepsilon_s} \quad \text{for} \ -x_p \le x < 0 \quad (8)$$

$$\mathcal{E}(x) = -\frac{d\Psi}{dx} = -\mathcal{E}_m + \frac{q}{\varepsilon_s} N_D = \frac{qN_A(x-x_n)}{\varepsilon_s} \quad (9)$$

$$\text{for} -x_p \le x < 0$$

where, $\mathcal{E}_m$ is the maximum field which exists at x = 0, and is given by:

$$\mathcal{E}_m = \frac{q}{\varepsilon_s} N_A x_p = \frac{q}{\varepsilon_s} N_D x_n \quad (10)$$

Integrating equations 8 and 9 over depletion region gives the total potential difference or built-in potential V_{bi};

$$V_{bi} = \frac{qN_A x_p^2}{2\varepsilon_s} + \frac{qN_A x_n^2}{2\varepsilon_s} = \frac{1}{2}\mathcal{E}_m W \quad (11)$$

where, W is the total depletion width and is given by:

$$W = x_p + x_n \qquad (12)$$

The x_p and x_n in the equation above represent the depletion layer width of the p-side and n-side, respectively.

Therefore, the total depletion layer width as a function of the built-in potential is given by;

$$W = \sqrt{\frac{2\varepsilon_s}{q}\left(\frac{N_A+N_D}{N_A N_D}\right)V_{ib}} \qquad (13)$$

However, for p-n junctions such as silicon and gallium arsenide, the width of neutral regions on p-side and n-side is negligible compared with the width of depletion region. Thus, the built-in potential is also negligible.

Furthermore, it should be noted that, the equations 3-13 are only valid for a p-n junction at room temperature without external bias. The depletion width of reverse bias is given by:

$$W = \sqrt{\frac{2\varepsilon_S(V_{bi}-V)}{qN_B}} \qquad (14)$$

where, V is the applied potential and it is positive for forward bias and negative for reverse bias, N_B is the lightly doped bulk concentration. Therefore, the electric field can be obtained by:

$$\varepsilon_m = \frac{qN_B W}{\varepsilon_s} \qquad (15)$$

Finally, the avalanche multiplication gain in *InAs* as described by Ker *et al.* [16] is exponentially rising, similar to that of HgCdTe APDs which can be calculated using equation given by [9]:

$$M = \exp(\alpha W) \qquad (16)$$

where, W is the width of the depletion region.

The ionization coefficient α can be obtained from the expression in equation 17 given by Marshall *et al.* [9].

$$\alpha = A\exp(-B/\varepsilon)^C \qquad (17)$$

where, ε is the electric field and A, B and C are constants.

2.3 Design Procedures

In order to design the advanced solid-state photomultiplier for the aforementioned applications, the following design procedures were adopted. Firstly, a p-n junction of InAs with an intrinsic layer in between the p and n-regions, now p-i-n InAs was designed. Constant doping concentrations for both acceptors and donor atoms per cm^3 was used and the depletion width, electric field as well as the multiplication gain were all calculated while varying reverse bias voltage from 0 - 10 volts. Secondly, the formation of series of p-i-n InAs (Advanced Solid-state photomultiplier). Likewise, the depletion width, electric field and multiplication gains were also computed while changing the reverse bias voltage from 0 -10 volts as in the initial step.

3. Results and Discussion

Electric field profile, impact ionization and avalanche multiplication gain of photodiodes can be aided using modelling. In this work, modelling and simulations of multiplication gain for the advanced photodetector were coded in the MATLAB Ra2016. Although the electric field profile simulated was low, it was sufficient enough such that electron drifting between p and n-regions undergoes impact ionization. Hence, the multiplication process will not result in junction breakdown or band-to-band tunneling since the electric field is less than 70 kV/cm.

Generally, for a computer program to perform a specific task, there must be a series of steps or model to be followed. Also, for this work, the steps followed by the program to execute its main task were summarized by the flow chart shown in Figure 3.1 below

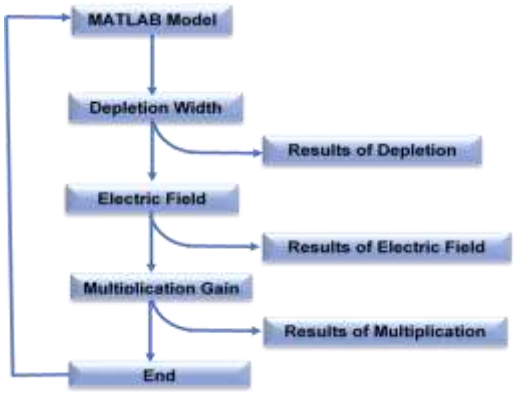

Figure 3.1: Program Flow Chart.

The model in Figure 3.1 above used the constants defined earlier such as electronic charge, doping concentration, material dielectric constant and varying applied reverse bias voltage (0 – 10V) to obtain the depletion width and display the results. The depletion width calculated is then used to obtain the electric field density and display the results as presented in Figures 3.2- 3.7.

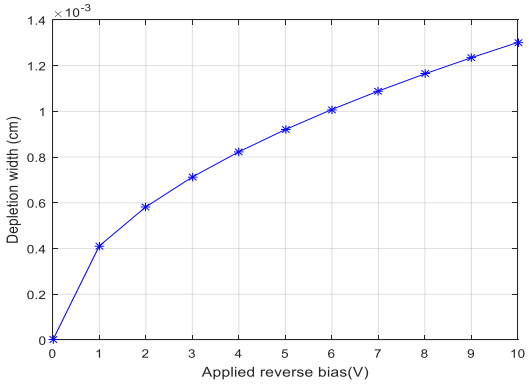

Figure 3.2: Depletion Width of p-i-n InAs

From the Figure 3.2 above, the results show an interesting increase in the width with increase in reverse bias voltage but is quite longer than what was reported in the literature for that of a simple p-n junction. This is due to the presence of intrinsic region (lightly doped semiconductor material) sandwiched in-between the p and the n-regions. However, from the results obtained, the width reached a maximum point at about 6 V and then remain steady even with increase in reverse bias voltage. Also, the results shown in Figure 3.3 below further show the variation of electric field density of the p-i-n InAs as function of the reverse bias voltage.

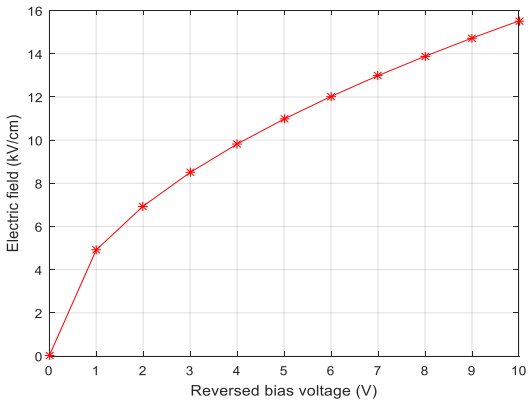

Figure 3.3: Electric Field of p-i-n InAs

From the figure above, it was observed that the electric field density increases with increase in the applied reverse bias voltage. Again, the high electric field density obtained, might be due to the intrinsic region sandwich in-between the p and n-regions which tends to increase the depletion width and at the same time the total number of charged carriers generated. Furthermore, multiplication gain of the single p-i-n InAs was also obtained while varying reverse bias voltage as shown in Figure 3.4 below.

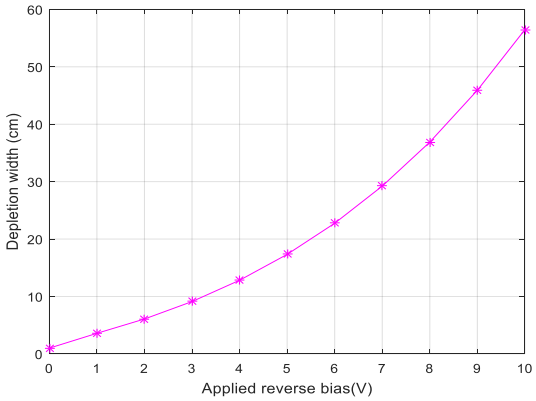

Figure 3.4: Gain of p-i-n InAs

From the results, an appreciable amount of gain of more than 10 was achieved before junction breakdown at about 4 V. This can be attributed to the increase in the depletion width resulting from the presence of intrinsic region sandwiched between p and n regions. Therefore, there are indications that increasing the depletion width can greatly increase the multiplication gain as well as the overall performance of the photomultiplier. Although it is very difficult to grow a junction of a single p-i-n InAs with depletion width greater than 5 µm, however, a longer depletion width, much greater than 5 µm, was achieved for the first time using a junction formed from a series p-i-n InAs (advanced photomultiplier) in Figure 3.5 below.

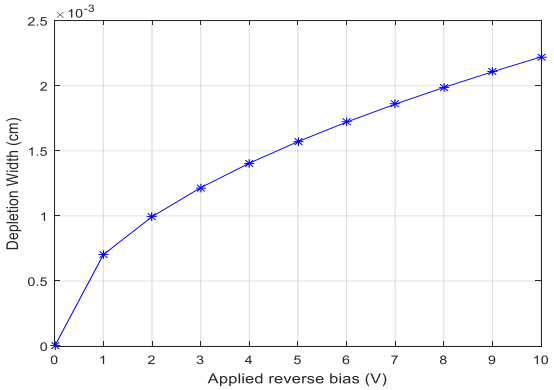

Figure 3.5: Depletion Width of Advanced Photomultiplier

For the advanced photomultiplier designed, the electric field obtained (Figure 3.6) also shows an increasing electric field with increase in reverse bias voltage as in single p-i-n InAs. However, the electric field obtained was far greater than what was achieved in the case of single p-i-n InAs design. In the case of advanced photomultiplier designed, the electric field obtained is sufficient enough to initiate avalanche multiplication, but also lower than 70 kV/cm to prevent junction breakdown or band-to-band tunneling.

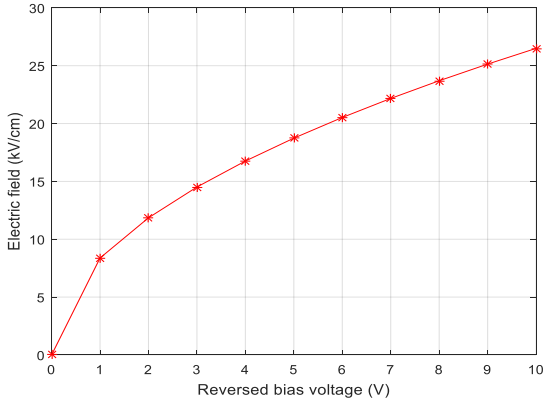

Figure 3.6: Electric Field of Advanced photomultiplier

Finally, the multiplication gains of the advanced photomultiplier designed is shown in Figure 3.6 below.

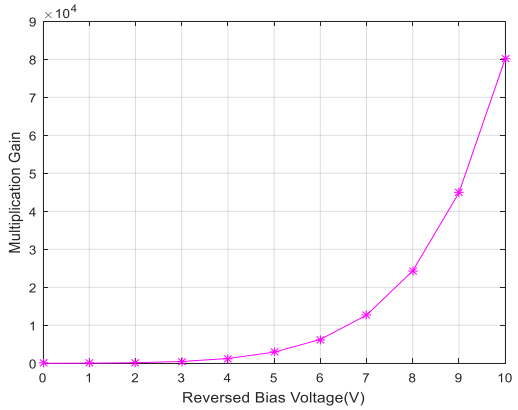

Figure 3.7: Gain of the Advanced Photomultiplier

It can be seen from these results (Figure 3.7) that, high gain was achieved for the first time from this novel design. However, the multiplication starts when the applied reverse bias voltage is above 2 volts. This is due to what is known as dead space [17] ("the minimum distance that a carrier must travel to attain an energy sufficient to cause impact ionization") as fully explained by Ong *et al* [18].

Overall, the results obtained from this new arrangement show an interesting performance when compared with what was obtained from Monte Carlo simulations by Satyanadh and Joshi [19] and that of Ong *et al* [18]. Similarly, the gain that was achieved in this study was far greater than was reported by Andrew *et al*., [9]. In all these previous studies, single junction was used in the design which is limited to particular depletion thickness of about 5 µm.

4. Conclusions

This current work has successfully designed an "advanced solid-state photomultiplier". A simple model was designed and coded in MATLAB Ra2016 to obtain the electric field profile, depletion width of both single p-i-n InAs and also that of the Advanced Solid-state photomultiplier designed. The results simulated were presented at constant doping concentration while varying the applied reverse voltage from 0 to10 V. The model showed an excellent agreement with both experimental and theoretically derived depletion width and data available from the literature. The simulated electron-initiated avalanche gain obtained from the photomultiplier designed showed a positive dependence on depletion width and doping concentration. A higher multiplication gain, greater than 1000, was achieved with the design. Thus, this new design could be used as a new first-class solid-state photomultiplier for various applications highlighted.

Nomenclature

K	Boltzmann Constant $(1.38 \times 10^{-23} m^2 kg S^{-2} K^{-1})$
M	Multiplication Gain (no unit)
N_D	Doping Concentration on p-side $(1 \times 10^{14} cm^{-3})$
N_A	Doping Concentration on n-side $(1 \times 10^{14} cm^{-3})$
q	Electron Charge $(1.6 \times 10^{-19} J)$
T	Temperature Kelvin (K)
V	Reverse Bias Voltage (V)
V_{ib}	Built-in potential (V)
W	Depletion Width (cm or µm)
x_p	Depletion Width of p-side (cm or µm)
x_n	Depletion Width of n-side (cm or µm)
α	Ionisation Coefficient (cm^{-1})
Ψ_p	Electrostatic Potential of p-side (V)
Ψ_n	Electrostatic Potential of n-side (V)
ε	Electric Field (V/cm or kV/cm)
ε_m	Maximum Electric Field (kV/cm)
ε_o	Permittivity of free Space $(8.85 \times 10^{-12} Fm^{-1})$
ε_r	Dielectric Constant (no unit)

References

1. Othman MA, Taib SN, Husain MN, Atfyi Z, Mohammed F. Reviews on Avalanche Photodiode for Optical Communication Technology. Journal of Engineering and Applied Sciences. 2014;9(1): 35–44. Available from: www.arpnjournals.com
2. Electronics Q. Random Response Time of Thin Avalanche Photodiodes. Optical and Quantum Electronics. 2017;36: 1155–1166. Available from: doi:10.1007/s11082-004-4626-7
3. Sandall I, Tan CH, Smith A, Gwilliam R. Planar InAs Photodiodes Fabricated using He ion Implantation. Optics Express. 2012;20(8): 8575–8583.
4. Singh A, Srivastav V, Pal R. HgCdTe Avalanche Photodiodes: A review. Optics and Laser Technology. 2011;43(7): 1358–1370. Available

from: doi:10.1016/j.optlastec.2011.03.009
5. Rahman A. A Review on Semiconductors Including Applications and Temperature Effects in Semiconductors. American Scientific Research Journal for Engineering, Technology, and Sciences. 2014;7: 50–70.
6. Ghosh KK. Multiplication Noise on Random Free Path Model In Short Avalanche Photodiodes Using The Monte Carlo Simulation. In: 4th International Conference of Electrical and Computer Engineering (ICECE). 2006. p. 19–21.
7. Marshall ARJ, Tan CH, Steer MJ, David JPR. Extremely Low Excess Noise in InAs Electron Avalanche Photodiodes. IEEE Photonics Technology Letters. 2009;21(13): 866–868.
8. Beck J, Scritchfield R, Sullivan B, Teherani J, Wan CF, Kinch M, et al. Performance and Modeling of the MWIR HgCdTe Electron Avalanche Photodiode. Journal of Electronic Materials. 2009;38(8): 1579–1592. Available from: doi:10.1007/s11664-009-0684-8
9. Marshall ARJ, Tan CH, Steer MJ, David JPR. Electron Dominated Impact Ionization and Avalanche Gain Characteristics in InAs Photodiodes. Applied Physics Letters. 2008;93(1): 2008–2010. Available from: doi:10.1063/1.2980451
10. Sandall IC, Ng JS, Xie S, Ker PJ, Tan CH. Temperature Dependence of Impact Ionization in InAs. Optics Express. 2013;21(7): 8630–8637. Available from: doi:10.1364/OE.21.008630
11. Mikhailova MP, Smirnova MM, Slobodchikov S V. Carrier Multiplication in InAs and InGaAs p-n Junctions and their Ionization Coefficients. Sov. Phys. Semicond. 1976;10(1): 509–513.
12. Brennan KF, Mansour NS. Monte Carlo Calculation of Electron Impact Ionization in Bulk InAs and HgCdTe. J. Appl. Phys. 1991;69(11): 7844–7847.
13. Marshall ARJ, David JPR, Tan CH. Impact ionization in InAs electron avalanche photodiodes. IEEE Transactions on Electron Devices. 2010;57(10): 2631–2638. Available from: doi:10.1109/TED.2010.2058330
14. Marshall ARJ. The InAs Electron Avalanche Photodiode. Advances in Photodiodes. Franco Dalla Betta: INTECH; 2011. Available from: /www.intechopen.com/books/advances-in-photodiodes/the-inas-electron-avalanche-photodiode
15. Sze SM. Semiconductor Devices: Physics and Technology. 2nd ed. New York: John Wiley & Sons; 2006. Available from: doi:10.1016/S0026-2692(82)80036-0
16. Ker PJ, Marshall A, Gomes R, David JP, Ng JS, Tan CH. InAs Electron-Avalanche Photodiodes : From Leaky Diodes to Extremely Low Noise Avalanche Photodiodes. IEEE. 2011. p. 276–277.
17. Ng JS, Tan CH, Member S, Ng BK, Hambleton PJ, David JPR, et al. Effect of Dead Space on Avalanche Speed. IEEE Transactions on Electron Devices. 2002;49(4): 544–549.
18. Ong DS, Li KF, Rees GJ, David JPR, Robson PN. A Simple Model to Determine Multiplication and Noise in Avalanche Photodiodes. J. Appl. Phys. 1998;83(6): 3426–3428. Available from: doi:10.1063/1.367111
19. Satyanadh G, Joshi RP. Monte Carlo Calculation of Electron Drift Characteristics and Avalanche Noise in Bulk InAs. Journal of Applied Phyics. 2002;91(3): 1331–1339. Available from: doi:10.1063/1.1429771